HHS Public Access

Author manuscript

Mol Carcinog. Author manuscript; available in PMC 2020 November 01.

Published in final edited form as:

Mol Carcinog. 2019 November ; 58(11): 2052–2064. doi:10.1002/mc.23097.

Inhibition of mutant Kras and p53 driven pancreatic carcinogenesis by atorvastatin: Mainly via targeting of the farnesylated DNAJA1 in chaperoning mutant p53

Dandan Xu[1], **Xin Tong**[1], **Leyu Sun**, **Haonan Li**, **Ryan D. Jones**, **Jie Liao**, **Guang-Yu Yang**[2]

Department of Pathology, Northwestern University Feinberg School of Medicine, 303 East Chicago Ave, Chicago, IL 60611

Abstract

Recent studies have indicated that using statins to inhibit the mevalonate pathway induces mutant p53 degradation by impairing the interaction of mutant p53 with DNAJA1. However, the role of the C-terminus of DNAJA1 with a CAAX box for farnesylation in the binding, folding and translocation of client proteins such as mutant p53 is not known. In the present study, we used a genetically engineered mouse model of pancreatic carcinoma and showed that atorvastatin significantly increased animal survival and inhibited pancreatic carcinogenesis. There was a dramatic decrease in mutant p53 protein accumulation in the pancreatic acini, PanINs and adenocarcinoma. Supplementation with farnesyl pyrophosphate, a substrate for protein farnesylation, rescued atorvastatin-induced mutant p53 degradation in pancreatic cancer cells. Tipifarnib, a farnesyltransferase inhibitor, mirrored atorvastatin's effects on mutant p53, degraded mutant p53 in a dose dependent manner, and converted farnesylated DNAJA1 into unfarnesylated DNAJA1. Farnesyltransferase gene knockdown also significantly promoted mutant p53 degradation. Co-immunoprecipitation either by an anti-DNAJA1 or p53 antibody confirmed the direct interaction of mutant p53 and DNAJA1 and higher doses of atorvastatin treatments converted more farnesylated DNAJA1 into unfarnesylated DNAJA1 with much less mutant p53 pulled down by DNAJA1. Strikingly, C394S mutant DNAJA1, in which the cysteine of the CAAX box was mutated to serine, was no longer able to be farnesylated and lost the ability to maintain mutant p53 stabilization. Our results show that farnesylated DNAJA1 is a crucial chaperone in maintaining mutant p53 stabilization and targeting farnesylated DNAJA1 by atorvastatin will be critical for inhibiting p53 mutant cancer.

Keywords

mutant p53; DNAJA1; farnesylation; pancreas; carcinogenesis; atorvastatin

[2]Corresponding Author: Guang-Yu Yang, MD, PhD, Department of Pathology, Northwestern University, Feinberg School of Medicine, 303 E. Chicago Ave, Ward 4-115, Chicago, IL 60611, Tel. (312) 503-0645, Fax. (312)503-0647, g-yang@northwestern.edu.

[1]These two authors are contributed equally

Conflict of interest

The authors have no conflicts of interest to declare.

1 INTRODUCTION

Pancreatic cancer is the 4th leading cause of cancer-related death in the United States and is expected to become the 2nd leading cause of cancer-related death by 2020. In 2019, an estimated 56,770 Americans will be diagnosed with pancreatic cancer and over 45,750 will die from the disease[1]. Only 9% of pancreatic cancer patients will survive more than five years and 74% die within the first year of diagnosis[1]. Point mutation of the Kirsten rat sarcoma viral oncogene homolog (KRAS) gene is the most frequent genetic alternation (found in more than 90% of human pancreatic cancer cases) and represents an early event in pancreatic carcinogenesis[2]. The TP53 tumor suppressor gene is also commonly mutated in human pancreatic cancer (60%), predominantly through missense mutations[3]. Therefore, targeting mutant p53 and its regulatory signaling is critical for the prevention and therapy of this lethal malignancy.

p53 has a crucial role in tumor suppression at least in part through its ability to regulate transcription of a number of downstream target genes involved in apoptosis, cell cycle arrest and metabolism[4]. Mutations in the TP53 gene are the most frequent genetic lesions in human tumors[5], and frequently occur at hotspot amino acids such as residues R175, G245, R248, R249, R273, and R282 in the DNA-binding domain[6]. This results in missense mutations with loss of function. Unlike wild-type p53, which is degraded rapidly in unstressed normal physiologic conditions, these missense mutations increase the stability of the p53 protein[7]. Consequently, these mutant versions of the p53 protein are commonly expressed at the high levels in cancer cells. Certain mutant p53 proteins not only abrogate their wild-type tumor suppressive functions, but frequently acquire pro-oncogenic activities that promote tumorigenesis, tumor cell survival, invasion and metastasis[8].

Targeting mutant p53 has emerged as a potential therapeutic strategy. The HSP90/HDAC6 chaperone machinery is highly activated in cancers compared to normal tissues and contributes to stabilizing mutant p53. Inhibition of Hsp90 causes degradation of mutant p53 and tumor regression in a mutant p53-dependent manner[9]. Recently, it has been shown that mevalonate kinase (MVK) stabilizes mutant p53 by inhibiting its ubiquitination by the CHIP (C-terminus of Hsc70-interacting protein) E3 ubiquitin ligase in a manner relying on DNAJA1, a Hsp40 family member[10]. Although previous studies have implicated E3 ubiquitin ligases (Mdm2 and CHIP) and heat shock proteins (Hsp70 and Hsp90) as critical regulators of mutant p53 stability in tumors[9–11], a complete understanding of the mechanisms underlying mutant p53 stability remains elusive.

The DnaJ proteins, also known as heat shock protein 40 (Hsp40), act as co-chaperones to the molecular chaperone DnaK (Hsp70), which is expressed abundantly in various tumors and is involved in mulitple cellular processes including DNA replication and transcription, protein folding and maturation, transport of polypeptides through membranes, assembly and disassembly of protein complexes, and cell signaling[12]. Human protein DnaJ subfamily A member 1 (DNAJA1) has critical roles in protein folding and spermatogenesis by controlling androgen receptor signaling[13,14]. DNAJA1 was also found to be involved in the mitochondrial import of proteins[15]. It is hypothesized that DNAJA1 may be implicated in importing apoptotic factors into the mitochondrial membrane during the biogenesis of

apoptosis[16]. Interestingly, DNAJA1 was significantly down-regulated in pancreatic cancer cells compared to normal cells, and was selected as a biomarker for pancreatic cancer to assess the effects of farnesyl protein transferase inhibitors[17,18]. A mechanistic study showed that overexpression of DNAJA1 appeared to activate DnaK protein by forming a JNK-suppressing complex, leading to hyperphosphorylation of c-Jun and a decrease in cell death in pancreatic cancer cells[19].

Although DNAJA1 is known to bind to mutant p53 and is implicated in misfolded protein degradation[10], little is known about the specific biological function for DNAJA1 farnesylation in the control of mutant p53 stability. Statins are inhibitors of 3-hydroxy-3-methylglutaryl-coenzyme A (HMG-CoA) reductase, which is a rate-limiting enzyme in the cholesterol/mevalonate pathway. Recent studies have suggests that statins may inhibit pancreatic cancer development and progression[20–22]. The mechanism by which statins produce anticancer effects remains elusive, though the mechanism could involve the inhibition of the mevalonate pathway, blocking the synthesis of intermediates important for protein prenylation and altering the expression of genes involved in lipid metabolism, which are important for pancreatic carcinogenesis[23]. In the present study, we continue our previously published work (in Molecular Carcinogenesis) on the use of atorvastatin to inhibit pancreatic carcinogenesis and increase survival in the *LSL-Kras^{G12D}-LSL-Trp53^{R172H}-Pdx1-Cre* pancreatic cancer mouse model[24]. We further demonstrate 1) a significant reduction of mutant p53 positive cells in early onset pancreatitis foci, mouse pancreas intraepithelial neoplasia lesion (mPanINs) and adenocarcinoma in in *LSL-Kras^{G12D}-LSL-Trp53^{R172H}-Pdx1-Cre* mice; 2) atorvastatin treatment in mouse pancreatic cancer cells (obtained from *LSL-Kras^{G12D}-LSL-Trp53^{R172H}-Pdx1-Cre* mice) induces degradation of mutant p53, resulting in cell cycle arrest and apoptosis; and 3) mechanistically, reduction of DNAJA1 farnesylation by atorvastatin or a farnesyl transferase inhibitor or by siRNA gene knockdown or or C394S mutant DNAJA1 (in which the cysteine of the CAAX box is mutated to serine, is no longer able to be farnesylated) impairs its binding and nuclear export of mutant p53, further degrading mutant p53. Our results provide a new mechanism by which atorvastatin prevents pancreatic cancer through targeting DNAJA1 farnesylation to induce mutant p53 degradation.

2 MATERIALS AND METHODS

2.1 Animal experiments

Pdx-1-Cre mice were kindly provided by Dr. Lowy (University of Cincinnati). *LSL-Trp53^{R172H}* and *LSL-Kras^{G12D}* mice were obtained from MMHCC, NCI/NIH and kindly provided by Dr. T. Jacks (MIT). C57BL/6J mice were purchased from the Jackson laboratory. All mice were genotyped in our laboratory following the protocols provided by the investigators[25]. The triple transgenic Kras^{G12D}-Trp53^{R172H}-Pdx-1-Cre mice (KPC ^{R172H}) were generated previously reported[26]. Mice were housed under pathogen-free conditions in the facilities of Laboratory Animal Services, Northwestern University. All studies were conducted in compliance with Northwestern University IACUC guidelines. The procedure and methods for atorvastatin with doses of 100 ppm and 200 ppm treated KPC ^{R172H} mice were published in Molecular Carcinogenesis[24].

2.2 Tissue preparation and histopathology

Mice were sacrificed by CO_2 asphyxiation. Organs were collected including the pancreas, liver, spleen, adrenals, kidney and lung. The numbers and sizes of tumors were recorded. Tumor volume was determined by the formula $V = 4/3\pi r^3$, where r was the average tumor radius obtained from three diameter measurements. Organs were fixed in 10% formalin for 24 hours, routinely processed and embedded in paraffin. 5 μm serial paraffin sections were obtained on poly-l-lysine-coated slides and stained with hematoxylin and eosin for histopathological analysis. Chronic pancreatitis, precancerous lesions and pancreatic tumors were analyzed histopathologically according to established criteria[27,28].

2.3 Immunohistochemistry

Immunohistochemical staining was carried out using an avidin-biotin-peroxidase method as previously described[24,26,29]. Endogenous peroxidase activity in paraffin-embedded tissue sections was quenched with 1% H_2O_2. Antigens were retrieved using a citrate buffer in the microwave. Horse serum was used to block nonspecific protein interactions. Slides were then incubated with primary antibody (1 μg/ml for Ki-67, or CM-5p p53 antibody, Vector Labs, Burlingame, CA), followed by the appropriate biotinylated secondary antibody and the avidin-biotin-peroxidase complex (Vector Labs, Burlingame, CA). 3,3-Diaminobenzidine (Sigma-Aldrich, St. Louis, MO) was used as the chromagen. Negative controls were established by replacing the primary antibody with phosphate-buffered saline and normal serum. Positive staining was indicated by the presence of a specific brown-colored precipitate. Positive cells and staining intensity were quantified using the Olympus BX45 microscope and DP70 digital Camera. The full image of each pancreas was snapped under 2.5X and 20X objective lens and saved with >2560 resolution image. Using ‘histogram analysis’ in the Photoshop program, specific staining intensity and percentage of positive staining cell number in total cells counted were measured for at least 10 defined areas/image including normal pancreas, acinar-ductal metaplasia, pancreatic intraepithelial neoplasia (PanIN) and pancreatic ductal adenocarcinoma (PDAC).

2.4 Cell culture, colony formation assay

The mouse pancreatic carcinoma cell line (PO3) was derived from PDAC KPC ^{R172H} mice. Cell lines were cultured in Dulbecco’s modified Eagle’s medium (DMEM) containing 10% fetal bovine serum, and 0.1% gentamicin and maintained at 37 °C with 5% CO_2. The human pancreatic carcinoma cell line (AsPC-1) was maintained in RPMI-1640 medium with 10% fetal bovine serum. A panel of human pancreatic cancer cells containing different p53 hotspot mutations (Panc 10.05, SU.86.86, BXPC-3, PANC-1 and MIA-PaCa-2) and SW1990 cell (containing WT p53) were cultured in their respective media according to ATCC website.

The colony formation assay was used to determine cell proliferation and tumorigenecity. Cells were seeded into 6 well culture plates (in triplicate) with 500 cells per well and incubated with the vehicle control (DMSO) or Atorvastatin in culture medium for 7 days. The colony was defined to consist of at least 50 cells. The inhibition percentage of cell colony formation was calculated.

2.5 Cell migration assay

Wound healing assay was performed to evaluate cell migration. Cells were scraped with 200μL sterile tips to make a straight scratch. Cell debris was removed by washing with PBS. Cells migration were photographed at 0, 16, 20, and 24 h, respectively. The width of the cell-free area was measured at each time point.

2.6 Invasive study using Matrigel Invasion Chambers approach

BioCoat matrigel invasion chambers (BD Biosciences, San Jose, CA) were used to investigate invasion activity. 10% fetal bovine serum in the lower chamber was used as a chemo-attractant. PO3 cell suspension (5×10^4 cells/well) in serum free DMEM medium was seeded in a matrigel invasion chamber and incubated for 22 hours. Invading cells on the underside of the chamber were fixed with 100% methanol, stained with Giemsa, and counted under the microscope. The number of cells that migrated through the membrane was determined by averaging 5 randomly selected fields of view. The result was expressed as the percent invasion through the matrigel matrix and membrane relative to the migration through the control membrane. Invasion index (expressed as the ratio of the percent invasion of a test cell over the percent invasion of a control cell) was also calculated by comparison to the control cells.

2.7 Cell fractionation and Western blot analysis

Cells were incubated in medium containing DMSO or chemicals for 24 h and 48 h. The following reagents were used in these studies: DL-Mevalolactone (M4667), DL-Mevalonic Acid 5-Phosphate (79849), Mevalonic acid 5-pyrophosphate (94259), Isopentenyl pyrophosphate (I0503), Geranyl pyrophosphate (G6772), Farnesyl pyrophosphate (F6892), Geranylgeranyl pyrophosphate (G6025), squalene (S3626) and tipifarnib (SML 1668). All were purchased from Sigma-Aldrich Co. LLC, and atorvastatin was purchased from Millipore. The medium was then removed and cells were washed, scraped and lysed on ice by overtaxing every 5 min for 30 min using radioimmunoprecipitation (RIPA) lysis buffer (Santa Cruz biotechnology, Santa Cruz, CA) containing 1% PMSF, 1% sodium orthovanadate, 1% protease inhibitor cocktail, 1% phosphatase inhibitor cocktails 2 and 3 (Sigma, St. Louis, MO). The extracts were centrifuged at 13,000 rpm for 10 min at 4 °C. The supernatant was collected. Protein concentrations were determined by the BCA assay (Thermo Fisher Scientific).

20 μg protein was loaded on SDS-PAGE and transferred to the Immun-Blot PVDF Membrane (Bio-Rad). The membrane was blocked with 5% non-fat dry milk in 1X TBST for 1 hour at room temperature and followed by incubation with the primary antibody solution overnight at 4 °C. The antibodies used were as follows: Rabbit polyclonal anti-p53 (FL-393) (1:200, Santa Cruz Biotechnology, Santa Cruz, CA), BCL2 (1:1000, Cell Signaling Technology, Danvers, MA), Caspase 9 (1:1000, Cell Signaling Technology), and cleaved Caspase-3 (1:1000, Cell Signaling Technology); mouse monoclonal anti-p53 (Pab 240) (1:200, Santa Cruz Biotechnology, Santa Cruz, CA), p53 (DO-1) (1:200, Santa Cruz Biotechnology), p21 (F-5) (1:200, Santa Cruz Biotechnology), cyclin D1 (M-20) (1:200, Santa Cruz Biotechnology), PCNA (NA03) (1:1000, EMD Millipore Corporation), and DNAJA1 (1:10000, Thermo Fisher Scientific); goat polyclonal anti-Lamin A/C (1:500,

Santa Cruz Biotechnology); 6XHis monoclonal antibody (1:2500, TaKaRa). Mouse anti-β-actin (1:10000, Sigma-Aldrich, St Louis, MO) and rabbit anti-vinculin (1:2000, Thermo Fisher Scientific) served as an internal control. The membrane was then washed with TBST and incubated with HRP-linked anti-rabbit (1:2000) or anti-mouse (1:2000) or anti-goat (1:5000) IgG and HRP-linked anti-biotin antibodies (1:2000, Cell Signaling Technology) for 1 hour at room temperature. The antibody-antigen complexes were detected using the 1X LumiGLO® chemiluminescent substrate (Cell Signaling Technology) according to the manufacturers' directions and the emitted light captured on X-ray film.

2.8 Flow cytometric analysis

Annexin V/ propidium iodide (PI) assay was used to analyze apoptosis. Cells were harvested and washed with PBS. 5 μL Annexin V-APC and PI (BD Pharmingen) was added to 100 μL 1×10^5 cells suspension in binding buffer and incubated for 15 minutes at room temperature in the dark. 400 μL binding buffer was then added. Finally, the treated cells were measured using the FACSCanto II instrument. 1×10^6 cells were harvested in 1 mL complete medium and stained with the Vybrant DyeCycle Violet stain (Invitrogen), and then incubated at 37°C for 30 minutes in the dark. Cell cycle assay was performed with flow cytometry and analyzed using FlowJo software.

2.9 Immunofluorescence

Cells were plated into 2 well chamber slides (Nunc™ Lab-Tek™ II) at a density of 1×10^5 cells/mL. After one day plating, cells were treated with DMSO or 40μM Atorvastatin for 24 h at 37°C. Cells were washed with PBS, fixed by 4% paraformaldehyde for 15 min, followed by permeabilization with 0.1% Triton X-100 in PBS for 10 min at room temperature, and blocked by 3% BSA in PBS containing 0.1% Triton X-100 for 1 h at room temperature. Cells were incubated overnight with anti-p53 (FL-393) antibody (1:50, Santa Cruz Biotechnology, Santa Cruz, CA) and anti-lamin A/C (4C11) antibody (1:200, Cell Signaling Technology), followed by incubation with Alexa-568 and Alexa-488 conjugated secondary antibodies (ThermoFisher Scientific) for 1 h at room temperature. Cells were then mounted with proLong™ gold antifade mountant with DAPI (Invitrogen). Immunofluorescence images were captured by NIKON A1R microscopy.

2.10 RNA Interference Experiment

A pool of several target-specific siRNA duplex targeting mouse FTβ mRNA and non-targeting control siRNA were purchased from Santa Cruz Biotechnology. siRNA for mouse and human DNAJA1 were from Millipore-Sigma. The transfection of siRNA into cells was performed by using Lipofectamine RNAiMAX (ThemoFisher Scientific) according to the manufacturer's instructions, cells were transfected for 24 h and followed by treatment with atorvastatin for another 24 h.

2.11 Co-Immunoprecipitation

Agarose-conjugated mutant p53 antibody was purchased from Santa Cruz Biotechnology. Agarose-conjugated DNAJA1 antibody was prepared by incubation of DNAJA1 antibody with protein A/G agarose beads on rotator for 4 h at 4 °C. Cell lysates were incubated with

agarose-conjugated antibody overnight on rotator at 4 °C. Samples were centrifuged at 2,000 × g for 2 min at 4 °C and the pelleted beads were washed 4 times with cold wash buffer supplemented with protease inhibitors. Finally, 25 μl loading buffer was added to each sample, followed by SDS-PAGE and Western Blot.

2.12 Plasmids, site-directed mutagenesis and DNA transfection

pCMV-Neo-Bam p53 R175H was a gift from Bert Vogelstein (Addgene plasmid # 16436) and human DNAJA1 cDNA was cloned into BamHI and NotI restriction sites of pcDNA5/FRT/TO HIS vector, a gift from Harm Kampinga (Addgene plasmid # 19545). DNAJA1 truncated mutants were generated by PCR of DNAJA1 cDNA and subsequently cloned into BamHI and NotI restriction sites of the pcDNA5/FRT/TO HIS vector. The C394S mutant of DNAJA1 was produced by QuikChange Multi Site-directed Mutagenesis kit (Agilent Technologies) to mutate codon 394 TGT (cysteine) to AGT (serine). All plasmids were confirmed by DNA sequencing. The transfection of plasmids into AsPC-1 cells was performed by using Lipofectamine 3000 (ThemoFisher Scientific) according to the manufacturer's instructions. Cells were first transfected with DNAJA1 siRNA to knock down endogenous DNAJA1 expression for 24 h and followed by co-transfecting p53 R175H plasmid and WT DNAJA1 or DNAJA1 mutants for another 24 h,

2.13 Statistical analysis

All experiments were repeated at least three times. For Western blot and cell image, a representative result was presented. The values were expressed as means ± standard deviation (SD). A probability value $p < 0.05$ (*$p < 0.05$, **$p < 0.01$ or ***$p < 0.001$) was considered to be statistically significant. Kaplan-Meier survival analysis was performed using SPSS software. Chi-square testing was used to analyze tumor incidence. Normally distributed data were analyzed using two-tailed Student's t-test, and nonparametric data were analyzed using the Mann-Whitney rank sum test.

3 RESULTS

3.1 Immunohistochemical analysis of mutant p53 in the pancreas of Pdx1Cre-K-ras^{G12D}-p53^{R172H} (called KPC^{172H}) mice treated with atorvastatin

Our prior publication confirmed that 100 and 200 ppm of atorvastatin significantly increased survival in KPC^{172H} mice with pancreatic carcinoma[24]. Histologic and immunochemical analyses showed that atorvastatin treatment resulted in a significant reduction in tumor volume, ki-67-labeled cell proliferation and protein farnesylation including Kras and DNAJA1[24]. The global gene expression profile demonstrated that a total of 132 genes were significantly modulated by atorvastatin including up-regulation of Waf1p21 (a wild-type p53 downstream signal), suggesting potential effects on mutant p53[24]. With histopathology, immunohistochemistry and Aperio Whole Slide Image analysis approaches, mutant p53 protein expression in these atorvastatin-treated pancreases was analyzed. Microscopic focus of early onset pancreatitis with or without mutant p53 accumulation in morphologically normal pancreatic parenchyma (acinar areas) was morphologically and immunohistochemically identified in the KPC^{172H} mice, as seen in Figure 1A –C. 100 and 200 ppm atorvastatin markedly reduced the p53 foci, as seen in Figure 1B and 1C. The

numbers of these p53 positive foci were quantitatively analyzed, expressed as p53 foci number/mm^2, and showed a significant reduction with atorvastatin treatment (Figure1 P). Similarly, the number of mutant p53 positive cells in mPanIN lesions (mPanIN 1 – 3, Figure 1D–L)) and pancreatic adenocarcinoma (Figure 1M–O) was also decreased in the mice treated with 100 and 200ppm atorvastatin, and quantitative analysis showed statistical significance ($p<0.001$, Figure 1Q).

3.2 Degradation of mutant p53 by atorvastatin mainly relies on specific effectors involved in mevalonate pathway

Our previous work demonstrated a dose-dependent inhibitory effect on pancreatic carcinoma cell growth after treatment with atorvastatin in mouse pancreatic carcinoma cell lines (PO3) derived from KPC^{172H} mice[24]. More recently, atorvastatin was also reported to reduce the protein level of mutant p53 in a dose-dependent manner without changing wild-type p53[10]. To determine whether the effect of atorvastatin on inhibiting pancreatic carcinogenesis in KPC^{172H} mice is related to its degradation of mutant p53, expression of mutant p53 protein was analyzed in mouse pancreatic carcinoma cell line (PO3) using a western blotting approach. We used two antibodies (sc-99 and sc-6243) to detect p53. Under non-denaturing conditions, sc-99 only detects mutant p53. However, sc-6243 can detect both WT and mutant p53. As illustrated in Figure 2A, atorvastatin reduced mutant p53 levels significantly at 24 and 48 h post treatment (sc-99 panel), but had no effect on wild-type p53 levels (sc-6243 panel, upper band).

Since atorvastatin inhibits HMG-CoA reductase activity (the rate-controlling enzyme of the mevalonate pathway in cholesterol synthesis) (Figure 2B)[20], to further examine effectors in the mevalonate pathway crucial for atorvastatin-induced mutant p53 degradation, we treated PO3 cells with 40 μM atorvastatin (the highest effective dose) in the presence or absence of 0.5 mM mevalonic acid (MVA) or mevalonate-5-phosphate (MVP) for 24 hour. Consistent with previous reports[10], Western blotting results showed that supplementation of either MVA or MVP completely rescued atorvastatin-induced mutant p53 degradation (Figure 2C). Furthermore, supplementation with MVA or MVP significantly reduced atorvastatin-induced apoptosis and cell cycle arrest (Figure 2D & 2E). These results indicate the importance of mevalonate pathway involvement in atorvastatin-induced mutant p53 degradation.

In contrast to previous reports[10], supplementation with mevalonic acid 5-pyrophosphate (MVA-5PP) also rescued atorvastatin-induced mutant p53 degradation in PO3 cells (Figure 2F). More interestingly, supplementation with Farnesyl pyrophosphate (FPP), and Geranylgeranyl pyrophosphate (GGPP) also rescued atorvastatin-induced mutant p53 degradation (Figure 2F). However, supplementation of squalene failed to rescue atorvastatin-induced mutant p53 degradation (Figure 2F).

3.3 The crucial role of DNAJA1 farnesylation in atorvastatin-induced mutant p53 degradation

Since supplementation of both FPP and GGPP are sufficient to rescue atorvastatin-induced mutant p53 degradation, but not squalene, this indicates that protein prenylation (including protein farnesylation) may play an important role in atorvastatin-induced mutant p53

degradation. Additionally, previous reports demonstrate that DNAJA1 interacts with mutant p53 and is responsible for maintaining mutant p53 protein stability[10]. DNAJA1 itself can be modified by protein farnesylation and therefore, we further tested whether DNAJA1 farnesylation is crucial for atorvastatin-induced mutant p53 degradation. To this end, we first treated PO3 cells with tipifarnib, a specific farnesyltransferase inhibitor. As illustrated in Figure 3A, tipifarnib alone can mirror atorvastatin's effect on mutant p53 and degraded mutant p53 in a dose dependent manner. At the same time, we found a decrease in farnesylated DNAJA1 levels and an increase in unfarnesylated DNAJA1 levels following tipifarnib treatment. We also knocked down the expression of farnesyltransferase subunit β, the essential subunit of the farnesyltransferase complex, in PO3 cells by siRNA, and found that even in the absence of atorvastatin treatment, knockdown of farnesyltransferase subunit β reduced mutant p53 protein levels (Figure 3B). As expected, knockdown of DNAJA1 itself also reduced mutant p53 levels, and atorvastatin treatment further reduced p53 levels (Figure 3C). Co-immunoprecipitation either by anti-DNAJA1 antibody or p53 antibody confirmed the direct interaction of mutant p53 and DNAJA1. Interestingly, higher doses of atorvastatin treatments converted more farnesylated DNAJA1 into unfarnesylated DNAJA1 with much less mutant p53 pulled down by DNAJA1, highlighting the critical role of DNAJA1 farnesylation for maintaining the level of mutant p53 (Figure 3D).

Because farnesyl transferase inhibitors or knockdown of farnesyl transferase expression may alter other farnesylated proteins, we further investigated directly whether farnesylation of DNAJA1 is required for mutant p53 stabilization. We used the p53-null human pancreatic cancer cell line (AsPC-1). We first knocked down endogenous DNAJA1 expression which was followed by co-transfection of the cells with mutant p53 R175H and WT DNAJA1, C394S mutant DNAJA1 or truncated DNAJA1. As illustrated in Figure 3 E and F, there was no endogenous p53 expression in AsPC-1 cells and transfection of cells with p53 R175H plasmid resulted in strong expression of mutant p53 protein and knockdown of endogenous DNAJA1 inhibited mutant p53 expression. However, co-transfection of WT DNAJA1 plasmid restored mutant p53 expression even after knockdown of endogenous DNAJA1, while C394S and truncated mutants failed to restore mutant p53 expression. More importantly, we found two bands of His tagged DNAJA1 (majority farnesylated DNAJA1 and a little unfarnesylated DNAJA1) after transfecting WT DNAJA1 into the cells, and only one unfarnesylated DNAJA1 band when cells were transfected with C394S mutant, strongly supporting our conclusion that DNAJA1 farnesylation is required for mutant p53 stabilization.

Together, these results indicate that not only is DNAJA1 is important for maintaining mutant p53 stability, but also that this crucial role of DNAJA1 is dependent on DNAJA1 protein farnesylation.

3.4 Atorvastatin-induced p53 degradation leading to induce apoptosis and cell cycle arrest in pancreatic cancer cells

To investigate whether a reduction in mutant p53 enhances wild-type p53 function, we treated PO3 cells with atorvastatin and carried out Western blotting to detect apoptosis related proteins (BCL2, cleaved caspase 9 and 3) and cell cycle related proteins (P21, Cyclin

D1 and PCNA). We found that atorvastatin decreased the protein levels of BCL2 and increased cleaved caspase 3 in a dose-dependent manner (Figure 4A). We also found that atorvastatin increased P21 protein expression and reduced Cyclin D1 and PCNA in a dose dependent manner (Figure 4B). To further evaluate the effects of atorvastatin treatment on apoptosis and cell cycle, we performed Annexin-V and PI staining followed by flow cytometry analysis. As shown in Figure 4C, after treatment of PO3 cells with atorvastatin at the indicated concentrations for 24 and 48 h, the percentage of Annexin-V positive cells (apoptotic cells) was increased in a dose dependent manner. Atorvastatin treatment also led to a significant increase of the sub-G1 fraction in PO3 cells at the 40 μM dose for 24 hour, and 10 to 40 μM dose for 48 hours (Figure 4D). These results demonstrate the induction of apoptosis and cell cycle arrest from mutant p53 degradation in mouse pancreatic cancer cells following atorvastatin treatment, possibly due to degrading mutant p53 and increasing wild-type p53 activity.

3.5 Atorvastatin inhibits cell migration and invasion *in vitro*

Cell migration and invasion are crucial steps for cancer metastasis. To evaluate if the degradation of mutant p53 induced by atorvastatin has an effect on the migratory ability of pancreatic cancer cells, we employed the wound healing assay, in which cells migrate into the wound place created by scratching with a pipette tip. After atorvastatin treatment, the migration abilities of PO3 cells were decreased in a dose dependent manner (Figure 5A). Moreover, the wound gaps of the PO3 cells treated with atorvastatin were still open at 24 hour while the control cells had almost closed the wound gap, indicating that atorvastatin treatment reduces migration abilities of PO3 cells. As an independent measure of cell motility, we further performed trans-well invasion assays to investigate the effect of atorvastatin treatment on the invasion ability of PO3 cells. As shown in Figure 5B, atorvastatin significantly decreased the invasion rate of PO3 cells in a dose-dependent manner compared to control cells. We also performed colony formation assays and found that atorvastatin inhibited PO3 cell growth significantly in a dose dependent manner (Figure 5C). Collectively, these data revealed that atorvastatin treatment inhibits migration and invasion of pancreatic cancer cells.

3.6 Subcellular distribution of mutant p53 after atorvastatin treatment

To investigate the effect of atorvastatin on cellular localization of mutant p53, confocal microscopy with immunofluorescence staining was performed. Figure 6 shows the nuclear location of mutant p53 highlighted by lamin A/C-stained nuclear membranes in the control PO3 cells. Atorvastatin-treated cells displayed both cytoplasmic and nuclear staining of mutant p53. DNAJA1 was distributed in the cytoplasm where it co-localized with cytoplasmic p53, indicating that atorvastatin may block the nuclear translocation of mutant p53.

3.7 Atorvastatin induces different mutant p53 degradation in a variety of human pancreatic cancer cell lines

Mutations in the TP53 gene represent the most frequent genetic lesions in human tumors, and the majority of the mutations span approximately 190 different codons localized in the DNA-binding domain of the protein. We wanted to determine if there were different effects

of atorvastatin on a panel of human pancreatic cancer cell lines containing a spectrum of p53 hotspot mutations. In addition to PO3 cells (carrying mutant p53 at R172H, equal to human R175H), as seen in Figure 7A, Panc 10.05, SU.86.86, and BXPC-3 cell lines carried a missense mutant p53 at sites of I255N, G245S, and Y220C, respectively exhibited a significant dose-dependent reduction of mutant p53 protein expression after atorvastatin treatment for 24 h, whereas there was no change in SW1990 (wild type p53), PANC-1 (mutant at R273H), and MIA-PaCa-2 (R248W) cells. It also showed that farnesyled DNAJA1 was reduced and unfarnesyled DNAJA1 was increased after atorvastatin treatment (Figure 7A). We further knocked down DNAJA1 expression by siRNA in SU.86.86 and BXPC-3 cells and found that reduced DNAJA1 alone could decrease mutant p53 expression in these cells (Figure 7B).

4 DISCUSSION

As a tumor suppressor, the TP53 gene functions mainly by inducing transcription of downstream target genes involved in the regulation of DNA repair, cell cycle arrest, senescence, apoptosis, and metabolism[4]. Loss of TP53 function results in uncontrolled cell proliferation, immortalization and eventually cancer development, which is supported by the evidence that more than half of human cancers have mutant p53. Mutant p53 can inhibit wild-type p53 activity by dominant-negative oligomerization with wild-type p53. More importantly, mutant p53 shows gain-of-function activities and functions like an oncogene. Targeting mutant p53 has been shown to reduce the malignant properties of cancer cells though the molecular mechanisms underlying mutant p53 stabilization and degradation are not fully understood.

Although the transcriptional regulation of p53 expression has been observed[30], regulation of p53 expression has historically been associated with mechanisms regulated primarily by post-transcriptional modifications of protein stability, p53 subcellular localization, and association with other proteins[31]. Recently, Parrales *et al* reported that DNAJA1, a member of the Hsp40 family, interacts with mutant p53 and is responsible for maintaining mutant p53 stability[10]. When cells are treated with statins, which inhibit the mevalonate pathway and prevents MVP production, reduced MVP inhibits the binding of mutant p53 to DNAJA1 but increases its interaction with CHIP, an ubiquitin ligase, resulting in mutant p53 degradation. However, there are remaining questions that need to be answered: How does MVP enhance the interaction between mutant p53 and DNAJA1 to stabilize mutant p53? DNAJA1 is often modified by protein farnesylation in cells, is DNAJA1 farnesylation involved in statin-induced (including atorvastatin) mutant p53 degradation? In the present study, we showed that DNAJA1 farnesylation plays a crucial role for mutant p53 stability and atorvastatin-induced mutant p53 degradation in pancreatic cancer cells. First, tipifarnib, a farnesyltransferase inhibitor, can mirror atorvastatin's effect on mutant p53, degraded mutant p53 in a dose dependent manner, and converted farnesylated DNAJA1 into unfarnesylated DNAJA1 at the same time. Second, knockdown of the expression of farnesyltransferase subunit β, the essential subunit of the farnesyltransferase complex, degraded mutant p53 in the absence of atorvastatin treatment. Third, co-immunoprecipitation showed that higher doses of atorvastatin treatments converted more farnesylated DNAJA1 into unfarnesylated DNAJA1 with much less mutant p53 pulled down

by DNAJA1. Fourth, C394S mutant DNAJA1 in which the cysteine of the CAAX box was mutated to serine, was no longer able to be farnesylated, and lost the ability to maintain mutant p53 stabilization. Fifth, supplementation with farnesyl pyrophosphate (FPP), the substrate for protein farnesylation, can rescue atorvastatin-induced mutant p53 degradation in pancreatic cancer cells. Finally, our previous work has demonstrated that atorvastatin inhibits cell growth in mouse pancreatic carcinoma cell lines derived from KPC^{172H} mice (containing p53^{R172H} mutation) and converts farnesylated DNAJA1 into unfarnesylated DNAJA1[24].

Protein prenylation is a post-translational modification by adding isoprenoid lipids to target proteins. This processing facilitates membrane interactions, promotes protein–protein interactions, and can also affect protein turnover[32]. Most prenylated proteins are post-translationally lipidated at a carboxyl-terminal CAAX motif, for which prenylation is initiated by the attachment of a 15-carbon (farnesyl) or a 20-carbon (geranylgeranyl) isoprenoid lipid to the Cys residue by either protein farnesyltransferase (FTase) or protein geranlygeranyltransferase-I (GGTase-I), respectively[32]. FTase and GGTase-I share a common α-subunit but have unique β-subunits that determine substrate specificity. Some proteins, such as DNAJA1 and prelamin A, are substrates for FTase, whereas others, such as RAP1A and RHOA, are substrates for GGTase-I[32]. We have found that in addition to farnesyl pyrophosphate (FPP), geranylgeranyl pyrophosphate (GGPP) can also rescue atorvastatin-induced mutant p53 degradation, suggesting that there are other molecular chaperones that can stabilize mutant p53 like DNAJA1, and may be subject to protein geranylgeranylation modification.

We report here that atorvastatin decreased mutant p53 expression in PO3 cells and further reduced cell growth, and we have previously reported that K-Ras undergoes farnesylation[24], thus the growth inhibition may be derived from reduced K-Ras farnesylation induced by atorvastatin.

Tumor-derived *TP53* missense mutations are generally clustered within the DNA-binding domain and rarely observed in the NH2 and COOH terminal. The majority of TP53 missense mutant proteins span approximately 190 different codons localized in the DNA-binding domain of the protein. Among them, 8 of these mutations account for “hotspot mutations” which represent ~28% of total p53 mutations and these alleles appear to be selected for preferentially in human cancers of many tissue types[6]. The main mutation we studied here - mouse p53^{R172H} (equivalent to humans p53^{R175H}) is one of the most common p53 mutation hotspots, and we wonder which other p53 mutants can also be degraded by atorvastatin. We chose a panel of 6 different human pancreatic cancer cells (wild-type p53 and different p53 mutation hotspots), and found that mutant p53 in 3 cell lines containing different p53 mutations other than p53^{R175H} also degraded after atorvastatin treatment, and farnesyled DNAJA1 was converted to unfarnesyled at the same time, indicating that DNAJA1 farnesylation is a common phenomenon in many pancreatic cancer cells and is responsible for the stability of multiple different mutant p53’s.

Functionally these missense mutant p53 proteins at the DNA-binding domain (residues 96–286) translate into a variety of impacts on its structure-function activity, which not only

perturbs the conformation of the binding surface thereby prompting its transition from the folded active wild-type state to an unfolded non-active state, but also promotes the oncogenic function[8]. In this study we considered that the interaction with intrinsic proteins such as heat shock proteins including DNAJA1 would be crucial to maintaining mutant p53 protein stability and contributing to carcinogenesis.

In the present study, we also found that atorvastatin-treated cells displayed both cytoplasmic and nuclear staining of mutant p53, whereas it was only found in nucleus in control cells, indicating that atorvastatin blocks the nuclear translocation of mutant p53. The C terminus of the p53 protein contains a cluster of several nuclear localization signals (NLSs) that mediate the migration of the protein into the cell nucleus[33]. However, increasing evidence also demonstrates that nuclear translocation can be modified by interactions with other proteins expressed in the cell, especially those proteins located in nuclear membrane. How atorvastatin blocks mutant p53 nuclear translocation remains elusive.

In summary, we have demonstrated that farnesylated DNAJA1 protein is a crucial chaperone for mutant p53 stability and nuclear translocation, and targeting the DNAJA1 farnesylation process by atorvastatin is an efficient approach to inhibiting pancreatic carcinogenesis via degrading oncogenic mutant p53 protein.

Acknowledgments

This study was supported by NIH R01 DK10776, CA172431, and CA164041 to Dr. Guang-Yu Yang.

Abbreviations:

CHIP	C-terminus of Hsc70-interacting protein
DMSO	dimethyl sulfoxide
DNAJA1	DnaJ subfamily A member 1
FPP	Farnesyl pyrophosphate
FTase	protein farnesyltransferase
GGPP	Geranylgeranyl pyrophosphate
GGTase-I	protein geranlygeranyltransferase-I
HMG-CoA	3-hydroxy-3-methylglutaryl-coenzyme A
MVA	mevalonic acid
MVA-5PP	mevalonic acid 5-pyrophosphate
MVK	mevalonate kinase
MVP	mevalonate-5-phosphate
PanIN	pancreas intraepithelial neoplasia lesion

PDAC	pancreatic ductal adenocarcinoma
PI	propidium iodide

References

1. Siegel RL, Miller KD, Jemal A. Cancer statistics, 2019. CA Cancer J Clin. 2019;69(1):7–34. [PubMed: 30620402]
2. Hruban RH, van Mansfeld AD, Offerhaus GJ, et al. K-ras oncogene activation in adenocarcinoma of the human pancreas. A study of 82 carcinomas using a combination of mutant-enriched polymerase chain reaction analysis and allele-specific oligonucleotide hybridization. Am J Pathol. 1993;143(2): 545–554. [PubMed: 8342602]
3. Scarpa A, Capelli P, Mukai K, et al. Pancreatic adenocarcinomas frequently show p53 gene mutations. Am J Pathol. 1993;142(5):1534–1543. [PubMed: 8494051]
4. Wade M, Li YC, Wahl GM. MDM2, MDMX and p53 in oncogenesis and cancer therapy. Nat Rev Cancer. 2013;13(2):83–96. [PubMed: 23303139]
5. Vogelstein B, Lane D, Levine AJ. Surfing the p53 network. Nature. 2000;408(6810):307–310. [PubMed: 11099028]
6. Petitjean AAM, Borresen-Dale AL, Hainaut P, Olivier M. TP53 mutations in human cancers: functional selection and impact on cancer prognosis and outcomes. oncogene. 2007;26(15):2157–2165. [PubMed: 17401424]
7. Brosh R, Rotter V. When mutants gain new powers: news from the mutant p53 field. Nat Rev Cancer. 2009;9(10):701–713. [PubMed: 19693097]
8. Freed-Pastor WA, Prives C. Mutant p53: one name, many proteins. Genes Dev. 2012;26(12):1268–1286. [PubMed: 22713868]
9. Alexandrova EM, Yallowitz AR, Li D, et al. Improving survival by exploiting tumour dependence on stabilized mutant p53 for treatment. Nature. 2015;523(7560):352–356. [PubMed: 26009011]
10. Parrales A, Ranjan A, Iyer SV, et al. DNAJA1 controls the fate of misfolded mutant p53 through the mevalonate pathway. Nat Cell Biol. 2016;18(11):1233–1243. [PubMed: 27775703]
11. Freed-Pastor WA, Mizuno H, Zhao X, et al. Mutant p53 disrupts mammary tissue architecture via the mevalonate pathway. Cell. 2012;148(1–2):244–258. [PubMed: 22265415]
12. Qiu XB, Shao YM, Miao S, Wang L. The diversity of the DnaJ/Hsp40 family, the crucial partners for Hsp70 chaperones. Cell Mol Life Sci. 2006;63(22):2560–2570. [PubMed: 16952052]
13. Terada K, Yomogida K, Imai T, et al. A type I DnaJ homolog, DjA1, regulates androgen receptor signaling and spermatogenesis. EMBO J. 2005;24(3):611–622. [PubMed: 15660130]
14. Terada K, Oike Y. Multiple molecules of Hsc70 and a dimer of DjA1 independently bind to an unfolded protein. J Biol Chem. 2010;285(22):16789–16797. [PubMed: 20363747]
15. Terada K, Kanazawa M, Bukau B, Mori M. The human DnaJ homologue dj2 facilitates mitochondrial protein import and luciferase refolding. J Cell Biol. 1997;139(5):1089–1095. [PubMed: 9382858]
16. Llambi F, Green DR. Apoptosis and oncogenesis: give and take in the BCL-2 family. Curr Opin Genet Dev. 2011;21(1):12–20. [PubMed: 21236661]
17. Patnaik A, Eckhardt SG, Izbicka E, et al. A phase I, pharmacokinetic, and biological study of the farnesyltransferase inhibitor tipifarnib in combination with gemcitabine in patients with advanced malignancies. Clin Cancer Res. 2003;9(13):4761–4771. [PubMed: 14581347]
18. Chow LQ, Eckhardt SG, O'Bryant CL, et al. A phase I safety, pharmacological, and biological study of the farnesyl protein transferase inhibitor, lonafarnib (SCH 663366), in combination with cisplatin and gemcitabine in patients with advanced solid tumors. Cancer Chemother Pharmacol. 2008;62(4):631–646. [PubMed: 18058098]
19. Stark JL, Mehla K, Chaika N, et al. Structure and function of human DnaJ homologue subfamily a member 1 (DNAJA1) and its relationship to pancreatic cancer. Biochemistry. 2014;53(8):1360–1372. [PubMed: 24512202]

20. Altwairgi AK. Statins are potential anticancerous agents (review). Oncol Rep. 2015;33(3):1019–1039. [PubMed: 25607255]
21. Chen MJ, Tsan YT, Liou JM, et al. Statins and the risk of pancreatic cancer in Type 2 diabetic patients--A population-based cohort study. Int J Cancer. 2016;138(3):594–603. [PubMed: 26296262]
22. Carey FJ, Little MW, Pugh TF, et al. The differential effects of statins on the risk of developing pancreatic cancer: a case-control study in two centres in the United Kingdom. Dig Dis Sci. 2013;58(11):3308–3312. [PubMed: 23864194]
23. Gong J, Sachdev E, Robbins LA, Lin E, Hendifar AE, Mita MM. Statins and pancreatic cancer. Oncol Lett. 2017;13(3):1035–1040. [PubMed: 28454210]
24. Liao J, Chung YT, Yang AL, et al. Atorvastatin inhibits pancreatic carcinogenesis and increases survival in LSL-KrasG12D-LSL-Trp53R172H-Pdx1-Cre mice. Mol Carcinog. 2013;52(9):739–750. [PubMed: 22549877]
25. Hingorani SR, Wang L, Multani AS, et al. Trp53R172H and KrasG12D cooperate to promote chromosomal instability and widely metastatic pancreatic ductal adenocarcinoma in mice. Cancer Cell. 2005;7(5):469–483. [PubMed: 15894267]
26. Li H, Yang AL, Chung YT, Zhang W, Liao J, Yang GY. Sulindac inhibits pancreatic carcinogenesis in LSL-KrasG12D-LSL-Trp53R172H-Pdx-1-Cre mice via suppressing aldo-keto reductase family 1B10 (AKR1B10). Carcinogenesis. 2013;34(9):2090–2098. [PubMed: 23689354]
27. Hruban RH, Adsay NV, Albores-Saavedra J, et al. Pathology of genetically engineered mouse models of pancreatic exocrine cancer: consensus report and recommendations. Cancer Res. 2006;66(1):95–106. [PubMed: 16397221]
28. Bai H, Li H, Zhang W, et al. Inhibition of chronic pancreatitis and pancreatic intraepithelial neoplasia (PanIN) by capsaicin in LSL-KrasG12D/Pdx1-Cre mice. Carcinogenesis. 2011;32(11):1689–1696. [PubMed: 21859833]
29. Seril DN, Liao J, Ho KL, Yang CS, Yang GY. Inhibition of chronic ulcerative colitis-associated colorectal adenocarcinoma development in a murine model by N-acetylcysteine. Carcinogenesis. 2002;23(6):993–1001. [PubMed: 12082021]
30. Noda A, Toma-Aiba Y, Fujiwara Y. A unique, short sequence determines p53 gene basal and UV-inducible expression in normal human cells. Oncogene. 2000;19(1):21–31. [PubMed: 10644976]
31. Lavin MF, Gueven N. The complexity of p53 stabilization and activation. Cell Death Differ. 2006;13(6):941–950. [PubMed: 16601750]
32. Wang M, Casey PJ. Protein prenylation: unique fats make their mark on biology. Nat Rev Mol Cell Biol. 2016;17(2):110–122. [PubMed: 26790532]
33. Shaulsky G, Goldfinger N, Ben-Ze'ev A, Rotter V. Nuclear accumulation of p53 protein is mediated by several nuclear localization signals and plays a role in tumorigenesis. Mol Cell Biol. 1990;10(12):6565–6577. [PubMed: 2247074]

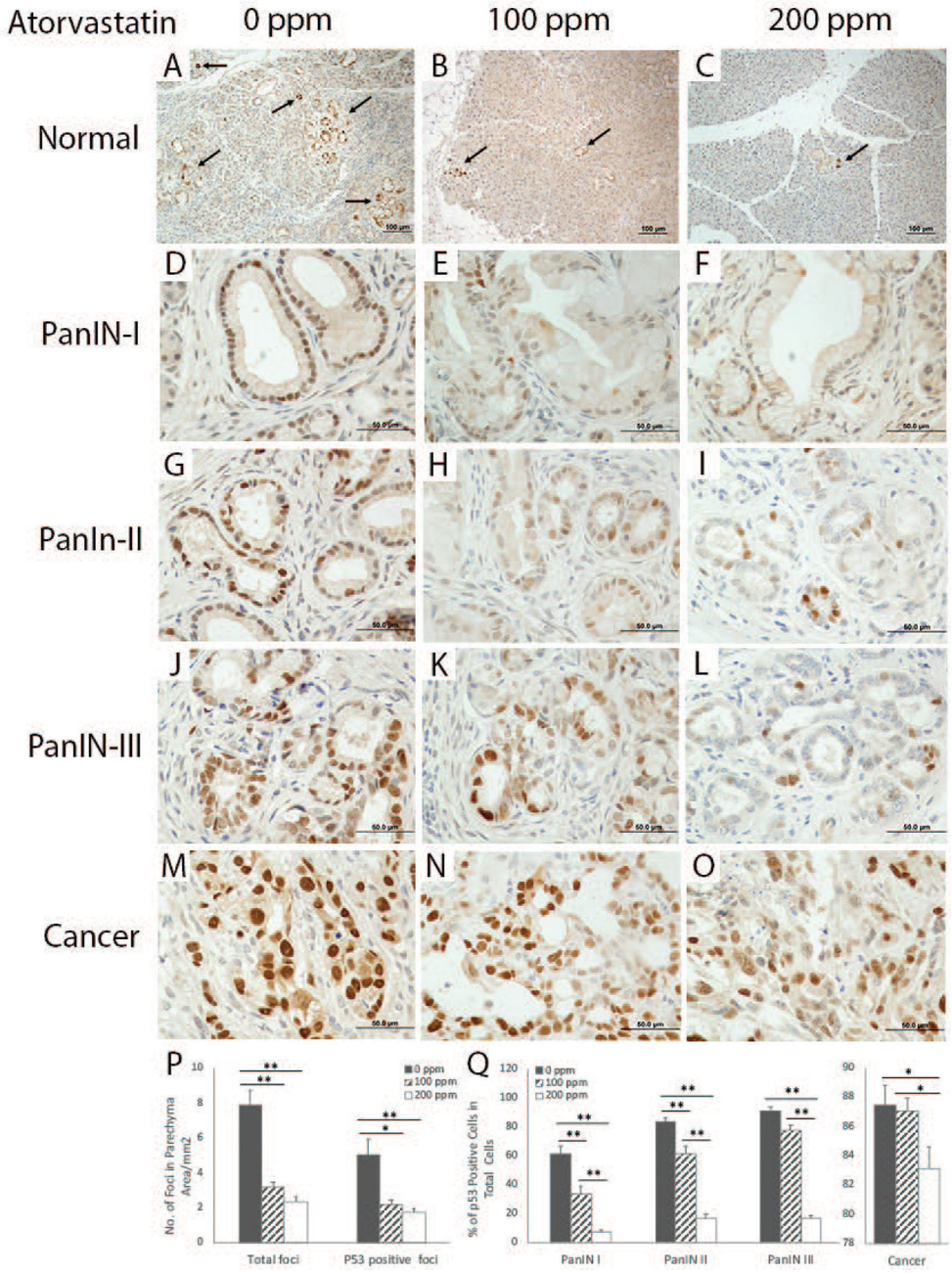

Figure 1. IHC analysis of mutant p53 protein accumulation in the pancreas, mPanINs and adenocarcinoma in KPC^{172H} mice. ***In morphologically normal pancreas,***
A - C) microscopic foci with mutant p53 protein accumulation in the morphologically normal pancreas; showing the pancreas from KPC^{172H} mice treated with atorvastatin at a dose of 0 ppm (A), 100 ppm (B) or 200ppm (C). ***In mouse pancreas intraepithelial neoplasia (mPanIN)*** from KPC^{172H} mice treated with atorvastatin at doses of 0, 100 or 200ppm**, D - F)** mPanIN 1; **G - I)** mPanIN 2; and (E), and **J - L)** mPanIN 3. (F). **M -O)** adenocarcinoma in KPC^{172H} mice. **P)** Histogram of the quantitative analysis of the number of microscopic foci with mutant p53 protein accumulation per area in morphologically

normal pancreas from KPC^{172H} mice treated with atorvastatin at doses of 0, 100 or 200ppm (*statistical significance P<0.01; **statistical significance P<0.001). **Q)** Histogram of the quantitative analysis for % of mutant p53 positive cells in mPanIN 1–3 and adenocarcinoma from KPC^{172H} mice treated with atorvastatin at doses of 0, 100 or 200ppm (*statistical significance P<0.01; **statistical significance P<0.001).

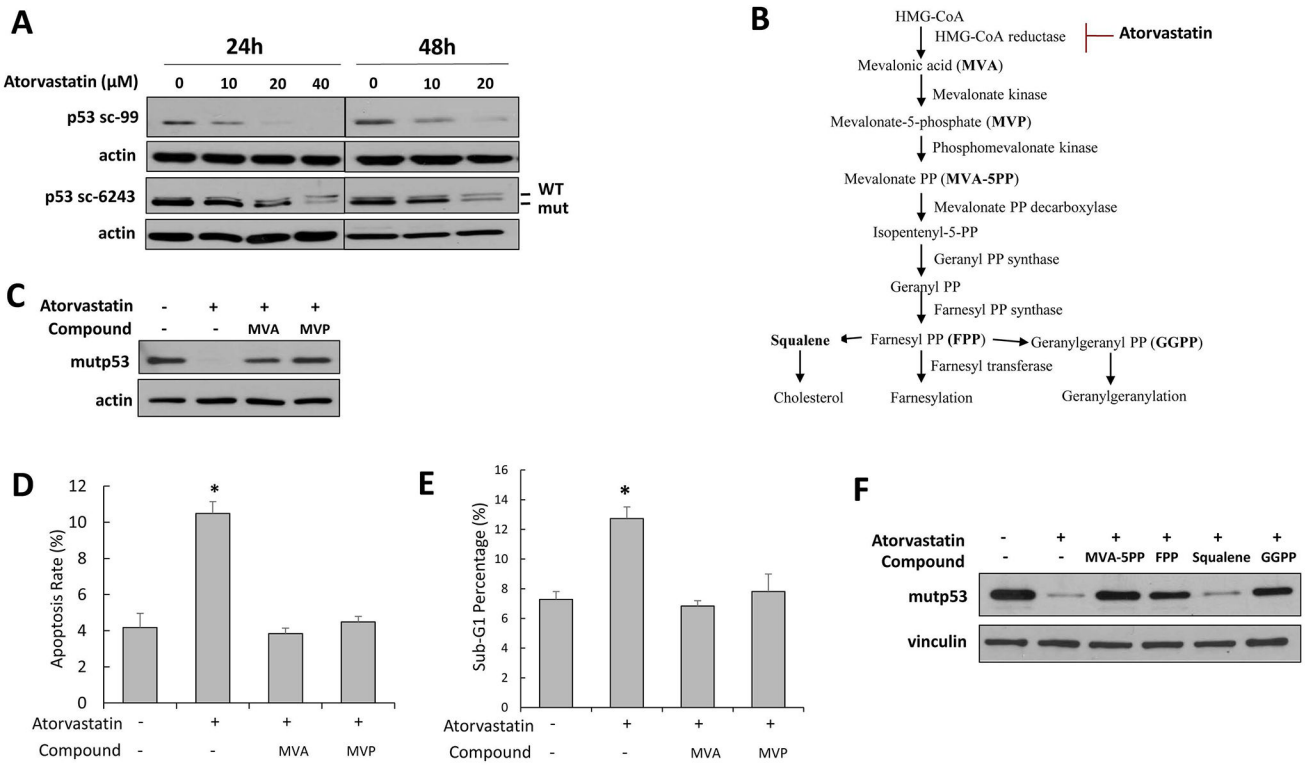

Figure 2. Atorvastatin-induced mutant p53 degradation and the involvement of the mevalonate pathway.

(A) Western blot for p53 and β-actin in PO3 cells treated with different doses of atorvastatin for 24 or 48 hours (B) Mevalonate pathway (C) Western blot for p53 and β-actin in PO3 cells treated with DMSO or atorvastatin (40 μM) in the presence or absence of 0.5mM mevalonic acid (MVA) or 0.5mM mevalonate-5-phosphate (MVP) for 24 hours (D and E) Cells were treated with atorvastatin (0 and 40 μM), 0.5mM MVA and 0.5mM MVAP for 24 hours. Flow cytometry analysis was performed to examine apoptosis and the cell cycle, respectively. Results were reported as mean ± SD (*P < 0.05 vs. control). (F) Western Blot for p53 and Vinculin in PO3 cells treated with atorvastatin (40 μM) in the presence or absence of 0.5mM MVA-5PP, 20 μM FPP, 20 μM GGPP and 200 μM squalene for 24 hours.

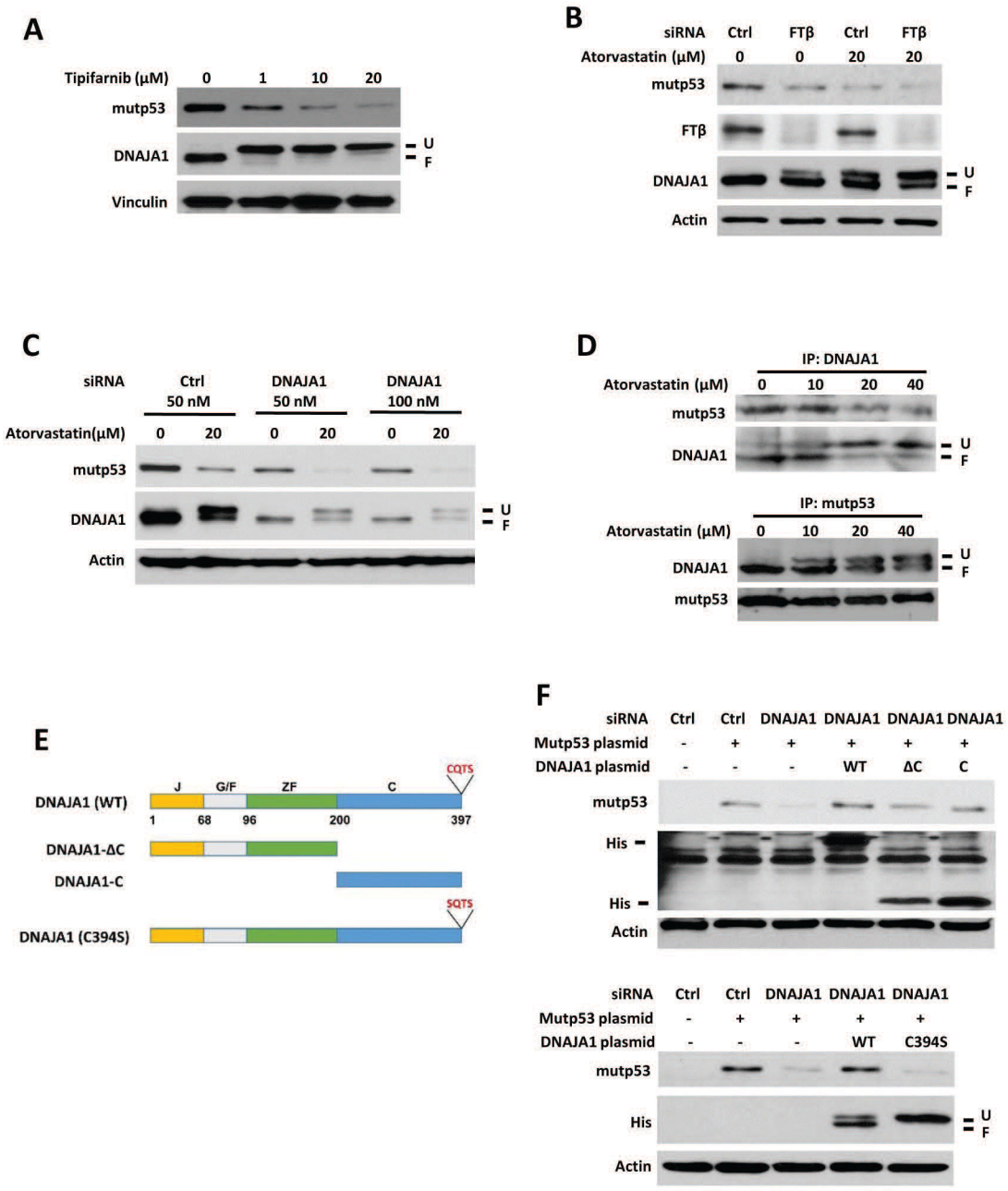

Figure 3. DNAJA1 farnesylation is important for atorvastatin-induced mutant p53 degradation.

(A) Western blot for mutant p53 and DNAJA1 in PO3 cells treated with different doses of tipifarnib. (B) Western blot for mutant p53, FTβ and DNAJA1 in PO3 cells after knockdown of FTβ by siRNA. (C) Western blot for mutant p53 and DNAJA1 in PO3 cells after knockdown of DNAJA1 by siRNA. (D) Co-immunoprecipitation either by anti-DnaJA1 antibody or p53 antibody to confirm the direct interaction of mutant p53 and DnaJA1. (E) Schematic diagram of His-tagged DNAJA1, truncation mutants and C394S mutant. The domain structure was designated as: J domain (J, 6–68), G/F-rich domain (G/F, 75–96), Zinc finger domain (ZF, 121–200), and C-terminal domain (C, 201–397). CAAX box (CQTS) was also present at the end of the C-terminal. (F) Western blot for mutant p53 and His-tag in

AsPC-1 cells transfected with DNAJA1 siRNA to knock down endogenous DNAJA1 expression for 24 h followed by co-transfecting p53 R175H plasmid and WT DNAJA1 or DNAJA1 mutants for another 24 h.

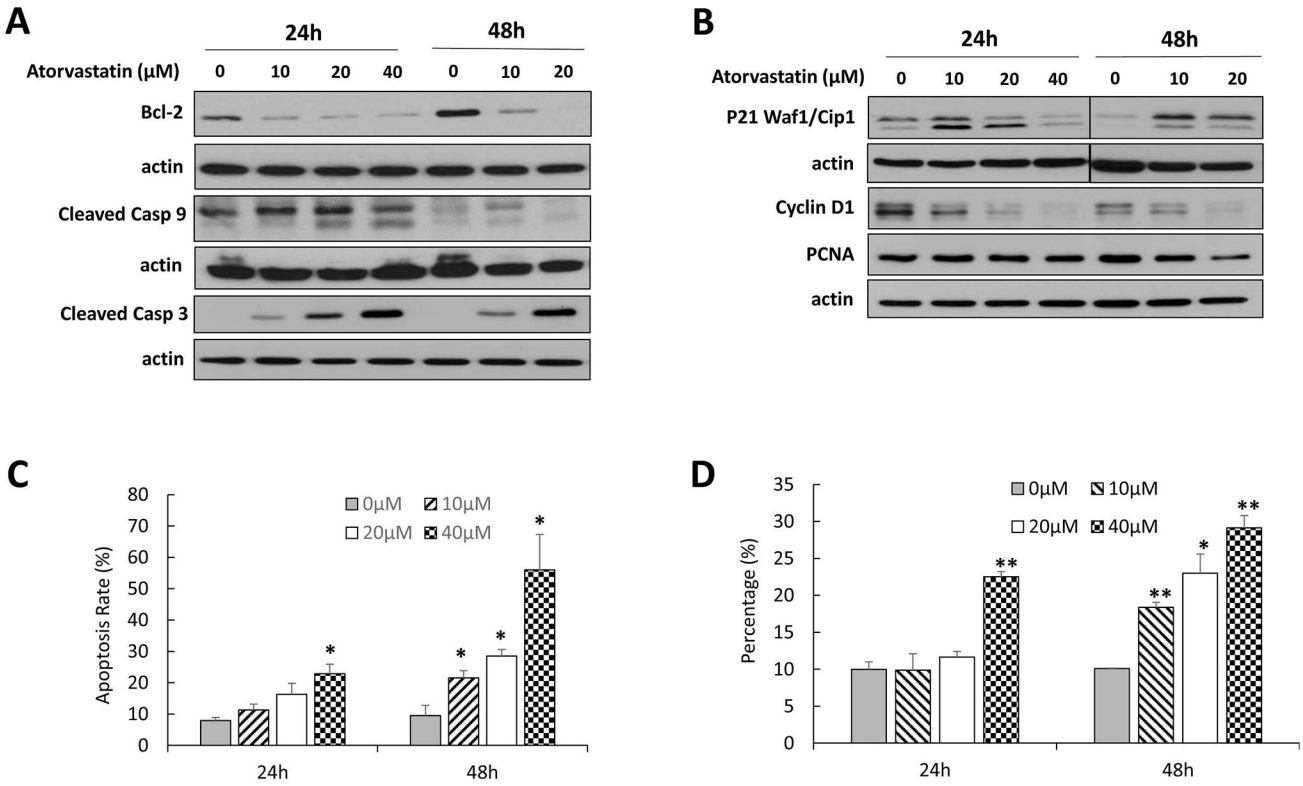

Figure 4. Atorvastatin induces apoptosis and cell cycle in PO3 cells.

(A) Western blot for BCL2, cleaved caspase 9, cleaved caspase 3 and β-actin in PO3 cells treated with DMSO or atorvastatin for 24 and 48 hours. (B) Western blot for p21 waf1, cyclin D1, PCNA and β-actin in PO3 cells treated with DMSO or atorvastatin for 24 and 48 hours. (C) PO3 cells were treated with 0, 10, 20, and 40 μM of atorvastatin for 24 and 48 hours, respectively, and followed by examining Annexin V and PI double staining to detect apoptosis by flow cytometry. Results were reported as mean ± SD. *P < 0.05 vs. control. (D) Flow cytometry analysis was performed to monitor cell cycle arrest in PO3 cells treated with different doses of atorvastatin for 24 and 48 hours, respectively. Histogram shows the percentages of sub-G1 cells. Results were reported as mean ± SD. *P < 0.05, **P < 0.01 vs. control.

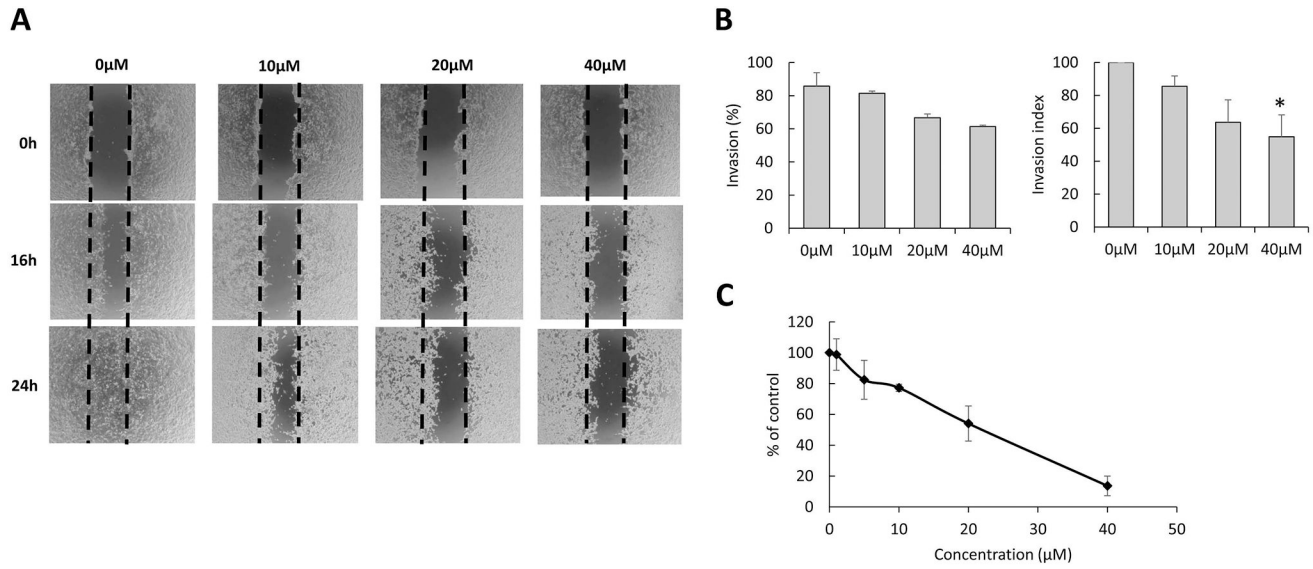

Figure 5. Assays for cell migration and invasion *in vitro*.

(A) Wound healing assay. Representative images for PO3 cells treated with 10, 20, and 40 μM of atorvastatin at 0, 16, 20 and 24 hours after wound formation. (B) Invasion assay. Cell invasion was analyzed by percentage of invasion and invasion index. (C) Colony formation assay. A dose-dependent inhibitory effect on cell growth by atorvastatin in PO3 cells. Results shown as mean ± SD (*P < 0.05) and all analysis were performed at 24 h after atorvastatin treatment.

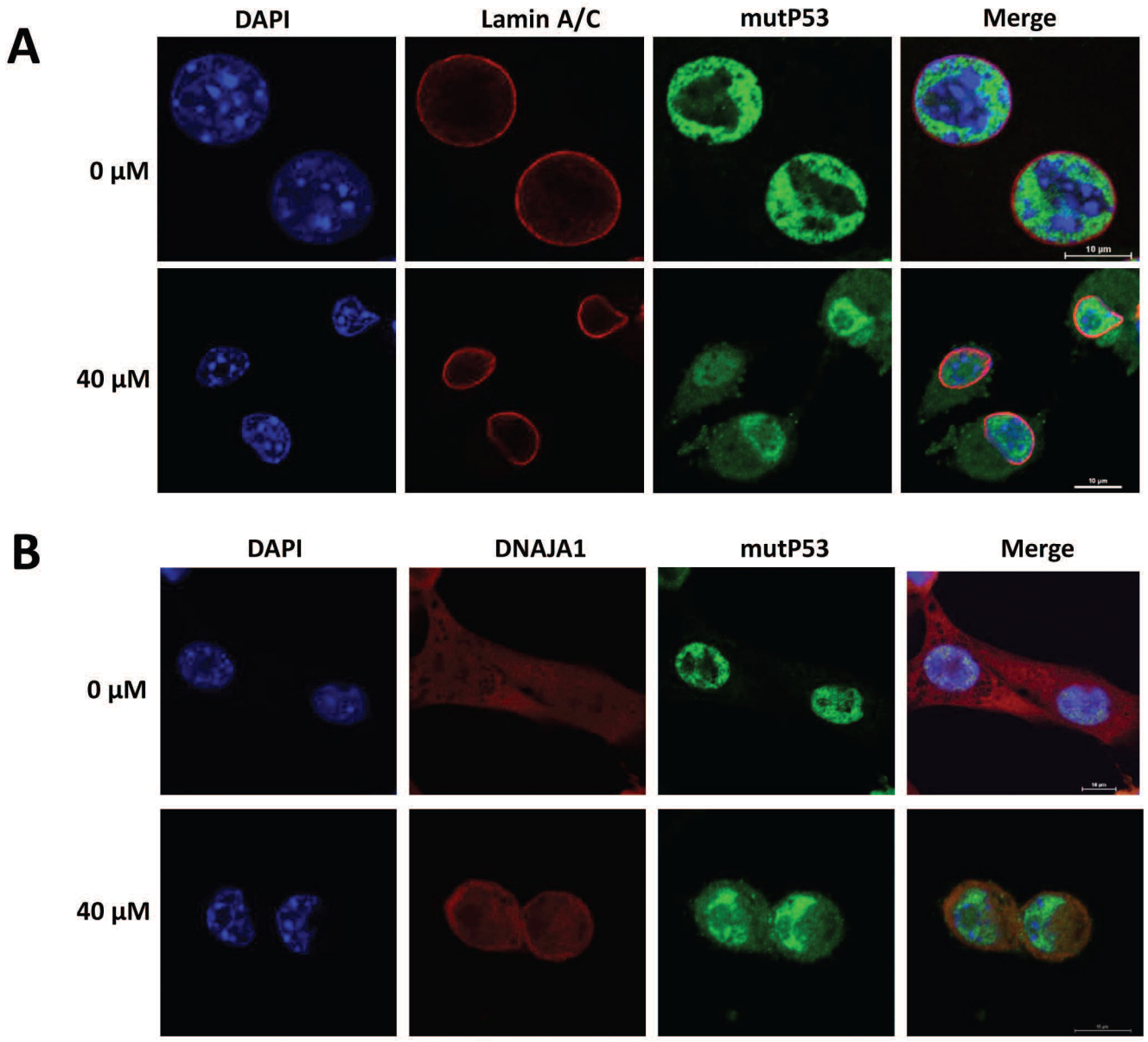

Figure 6. Subcellular localization of mutant p53 in PO3 cells after atorvastatin treatment.
Cells were grown on chamber slides and fixed with 4% paraformaldehyde in PBS. (A) Immunostaining with lamin A/C (red), p53 (green), and DAPI (blue). (B) Immunostaining with DNAJA1 (red), p53 (green), and DAPI (blue).

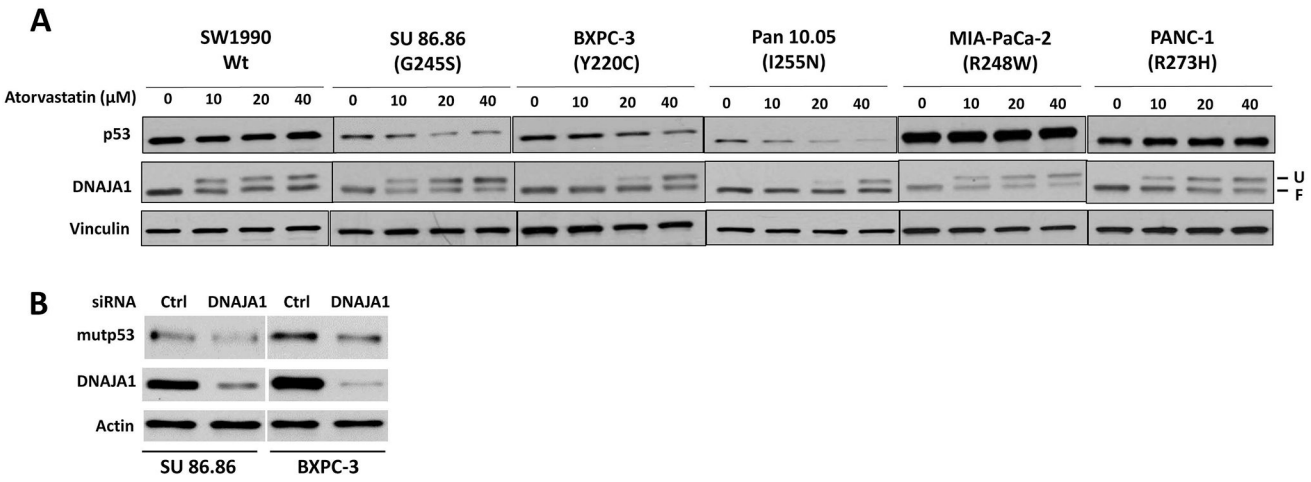

Figure 7. Effects of atorvastatin on a panel of human pancreatic cancer cells containing different p53 hotspot mutations.

(A) Western blot for p53 and DNAJA1 in cells treated with different doses of atorvastatin. (B) DNAJA1 was knocked down by siRNA in SU.86.86 and BXPC-3 cells, and mutant p53 was detected by Western blot.